

# Geometric-Facilitated Denoising Diffusion Model for 3D Molecule Generation

Can Xu<sup>1,2\*†</sup>, Haosen Wang<sup>3,2\*</sup>, Weigang Wang<sup>1†</sup>, Pengfei Zheng<sup>2</sup>, Hongyang Chen<sup>2‡</sup>,

<sup>1</sup>Zhejiang Gongshang University

<sup>2</sup>Zhejiang Lab

<sup>3</sup>Southeast University

leoxc1571@163.com, haosenwang@seu.edu.cn, wangweigang@zjgsu.edu.cn, zpf2021@zhejianglab.com, dr.h.chen@ieee.org

## Abstract

Denoising diffusion models have shown great potential in multiple research areas. Existing diffusion-based generative methods on *de novo* 3D molecule generation face two major challenges. Since majority heavy atoms in molecules allow connections to multiple atoms through single bonds, solely using pair-wise distance to model molecule geometries is insufficient. Therefore, the first one involves proposing an effective neural network as the denoising kernel that is capable to capture complex multi-body interatomic relationships and learn high-quality features. Due to the discrete nature of graphs, mainstream diffusion-based methods for molecules heavily rely on predefined rules and generate edges in an indirect manner. The second challenge involves accommodating molecule generation to diffusion and accurately predicting the existence of bonds. In our research, we view the iterative way of updating molecule conformations in diffusion process is consistent with molecular dynamics and introduce a novel molecule generation method named Geometric-Facilitated Molecular Diffusion (GFMDiff). For the first challenge, we introduce a Dual-Track Transformer Network (DTN) to fully excavate global spatial relationships and learn high quality representations which contribute to accurate predictions of features and geometries. As for the second challenge, we design Geometric-Facilitated Loss (GFLoss) which intervenes the formation of bonds during the training period, instead of directly embedding edges into the latent space. Comprehensive experiments on current benchmarks demonstrate the superiority of GFMDiff.

## Introduction

Recent advances in deep generative methods, especially diffusion-based methods (Ho, Jain, and Abbeel 2020; Song and Ermon 2019; Song et al. 2021), have greatly propelled research in generative artificial intelligence across various domains. In line with the development trend of generative methods, mainstream approaches in the field of molecule discovery have undergone a transformation from previous generative methods to diffusion-based methods, and from designing 2D graphs to 3D conformations. However, there are

two major challenges in 3D molecule generation. The first one involves predicting accurate and stable molecule conformations while the other entails fully utilizing geometric information to facilitate the generation of discrete graph structures. In this paper, we propose **Geometric-Facilitated Molecular Diffusion** (GFMDiff), a *de novo* 3D molecule generative method that addresses the aforementioned challenges. GFMDiff is capable of generating accurate 3D geometries while tackling the discrete nature of graphs.

*De novo* molecule generation involves generating valid, novel, and stable molecules. To address the quest for equivariance of generated 3D conformations, several diffusion-based methods (Hoogeboom et al. 2022; Huang et al. 2023) model molecules indirectly through atomic distances, which directly reflect the strength of interatomic forces. However, earlier methods (Hoogeboom et al. 2022) did not address the complex interatomic relationships among multiple atoms. While the others (Huang et al. 2023) simply use a threshold to distinguish the influence caused by chemical bonds and interatomic forces, regardless of specific atom and bond types. However, apart from few atoms like fluorine, chlorine, and bromine, majority heavy atoms in molecules allow connections to other atoms through single bonds. Therefore, we consider simply using pair-wise distances to model molecule geometries is far from sufficient. Recent research (Yuan et al. 2023) also indicates that the contribution of bond angles on molecular learning is equivalent to pair-wise distances. Only a limited number of methods make full use of spatial information. Additionally, since molecular diffusion methods only act on points cloud, traditional graph convolutions are unable to discriminate the importance of different atoms. In light of these challenges, we design a novel dual track molecular learning framework named **Dual-Track Transformer Network** (DTN). By integrating global transformer architecture, DTN serves as the denoising kernel to comprehensively capture spatial geometric information.

Given the excellent performance of diffusion models on continuous data, majority of the models for molecule graph generation adopt the diffusion and denoising approach on Cartesian coordinates and features, followed by graph generation based on predefined rules instead of directly predicting the existence of bonds. The manner in which graphs are generated indirectly can potentially lead to degradation in stabilities and validity of generated samples. To make diffusion

\*This work is done during internship at Zhejiang Lab.

†Equal contribution, co-first author.

‡Correspond to Hongyang Chen.

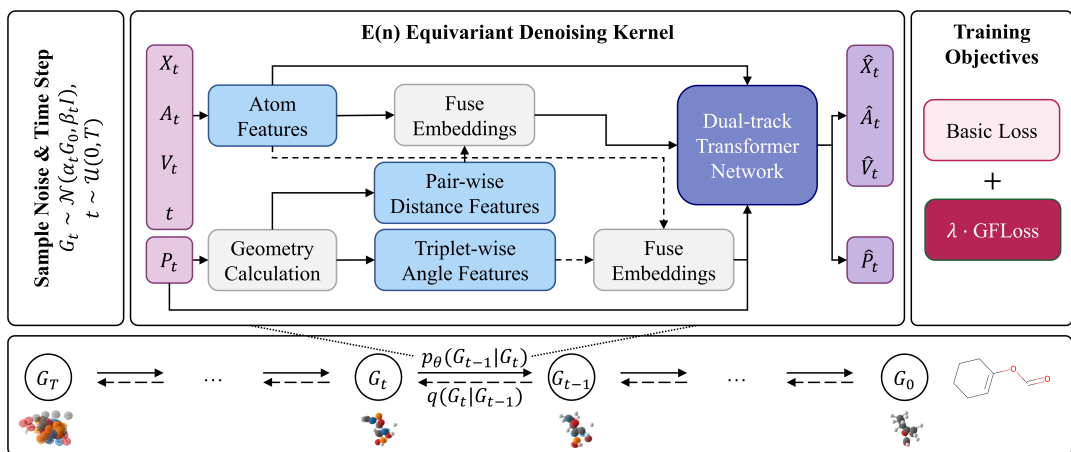


Figure 1: An overview of GFMDiff. For each noise sample at arbitrary time step, the denoising kernel predicts atom types, valencies, and coordinates through the DTN. A loss term named GFLoss that intervenes in the formation of bonds is added to the training objective as well.

model applicable to multimodal data of molecules, several studies (Niu et al. 2020; Vignac et al. 2023a,b) introduce adjacency matrices to diffusion and denoising process. However, embedding graphs and edges into models leads to the rise of computational cost. In our research, we view diffusion model as a process that iteratively update atom information according to local multi-body interatomic relationship at each time step. Accurate feature learning assists on precise predictions of molecule conformations. In order to predict spot on molecule conformations, we devise a way by mitigating the gap between embeddings and local geometries during training. In this paper, we actively intervene the formation of graphs with a delicately designed loss function named **Geometric-Facilitated Loss** (GFLoss).

In this paper, we present **Geometric-Facilitated Molecular Diffusion** (GFMDiff) for 3D molecule generation. In contrast to previous methods that primarily learn atom representations based-on pair-wise distances, we manage to effectively incorporate triplet-wise geometric information along with pair-wise distances into molecular learning. Most studies directly generate point clouds and subsequently complete 3D graph structures based on predefined rules. However, this approach suffers from two major constraints. Firstly, the indirect manner of graph generation causes degradation of stability and validity of samples. Secondly, traditional graph convolutions are not sufficient enough to distinguish local and global information. To address the first constraint, we proactively guide the formation of bonds during the training phase with a exquisite loss function named **Geometric-Facilitated Loss** (GFLoss). As for the second constraint, we introduce **Dual-Track Transformer Network** (DTN), a global transformer-based neural network, to promote comprehensive geometric learning and local feature learning. Main contributions of this paper are as follows:

- Comprehensive utilization of spatial information to capture multi-body interactions among atoms, which is crucial for molecular learning and stabilities of generated

samples.

- Introduction of a carefully designed GFLoss to facilitate the formation of bonds, addressing the discrete nature of graphs in an efficient manner.
- Proposal of DTN as an alternative to global graph convolutions which enables the model to capture both global and local information effectively.

## Related Works

### Diffusion Models

Diffusion-based methods arouse wide attention due to their excellent performance in generative tasks across multiple fields, such as computer vision (Avrahami, Lischinski, and Fried 2022; Ho et al. 2022; Cai et al. 2020; Luo and Hu 2021), natural language processing (Hooeboom et al. 2021; Savinov et al. 2022), as well as various interdisciplinary tasks (Shabani, Hosseini, and Furukawa 2023; Lei et al. 2023) et al.

The formation of human motion skeletons share similarities to molecules, as both are represented by point clouds connected by edges. The difference is that human motion generation does not require predictions of edges. Building upon DDPMs, MoFusion (Dabral et al. 2023) employs U-Net (Ronneberger, Fischer, and Brox 2015) as the backbone for the denoising kernel in motion sequence synthesis. Apart from applications on continuous data, many research efforts are devoted to discrete data generation. EDP-GNN (Niu et al. 2020) introduce Score SDEs, a learning paradigm of diffusion models, to the generation of discrete graph adjacency matrices.

### Molecule Generation

Over the past years, various generative methods have been employed for molecule generation, including variational autoencoders (VAEs) (Kingma and Welling 2022), normalizing flows (NFs) (Dinh, Krueger, and Bengio 2015),

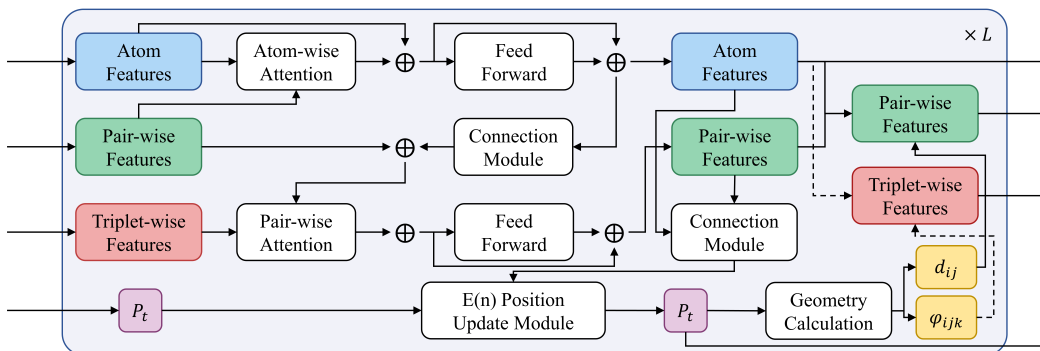


Figure 2: The illustration of Dual-Track Transformer Network (DTN). The atom-pair track and pair-triplet with multi-head attention modules update atom and pair-wise features, respectively. The pair-wise and triplet-wise features are further fused with the latest position information.

and generative adversarial network (GANs) (Goodfellow et al. 2014). In order to generate 3D molecules, G-SchNet (Gebauer, Gastegger, and Schütt 2019) adopts an autoregressive model with a rotation invariant and local symmetrical network to add atoms incrementally. In the field of computational chemistry, diffusion models, well-suited for continuous data, are first introduced to conformation generation that takes molecule graphs as input and only operates on atom coordinates. EDM (Hoogeboom et al. 2022) and MDM (Huang et al. 2023) convert discrete atom features into one-hot format to make generated samples more chemical feasible and stable. In order to generate edges without relying on predefined rules, Digress (Vignac et al. 2023a) and MiDi (Vignac et al. 2023b) propose discrete diffusion techniques.

## Preliminaries

### Denosing Diffusion Probabilistic Models

Diffusion models have garnered considerable attention as powerful generative models. By learning the denosing kernel of the reverse process, these models are able to uncover underlying distributions of noisy samples. Given a piece of data, the forward process, treated as a Markov chain, gradually adds Gaussian noises for  $T$  times to with learnable parameters controlling the strength of noises. During the generative process, the model reverses the noise back to the original distribution of real data.

**Diffusion Process** Let  $G_t (t = 0, 1, \dots, T)$  denotes distributions of molecule geometry information and  $\beta_t \in (0, 1), t = 0, 1, \dots, T$  denote the variance schedule of the Markov chain. Therefore we have the posterior distribution of  $G_t$ :

$$q(G_{1:T}|G_0) = \prod_{t=1}^T q(G_t|G_{t-1}), \quad (1)$$

$$q(G_t|G_{t-1}) = \mathcal{N}(G_t; \sqrt{1 - \beta_t}G_{t-1}, \beta_t I). \quad (2)$$

As time step  $t$  rises, the variance schedule  $\beta_t$  smoothly transits from 0 to 1, which means more noise is added to the original data distribution. Let  $\bar{\alpha}_t = \prod_{s=1}^t \alpha_s = \prod_{s=1}^t (1 - \beta_s)$ , the distribution of sample data

$$q(G_t|G_0) = \mathcal{N}(G_t; \sqrt{\bar{\alpha}_t}G_0, (1 - \bar{\alpha}_t)I). \quad (3)$$

**Denosing Process** During the denosing process, the model manages to reconstruct the original geometry information by learning Markov kernels  $p_\theta(G_{0:T-1}|G_T) = \prod_{t=1}^T p_\theta(G_{t-1}|G_t)$  close to the actual reverse process  $q(G_{t-1}|G_t)$ . The distribution of learned parameterized dynamics at each time step is:

$$p_\theta(G_{t-1}|G_t) = \mathcal{N}(G_{t-1}; \mu_\theta(G_t, t), \sigma_t^2 I), \quad (4)$$

where  $\mu_\theta(G_t, t)$  is the neural network to approximate the means and  $\sigma_t^2 = \frac{(\beta_t - \beta_{t-1})\beta_{t-1}}{(1 - \beta_{t-1})\beta_t}$  is the predefined variance schedule. Initially, the  $p_\theta(G_t)$  is sampled from a standard Guassian distribution. Then the geometry information and atom features get polished over the reverse process iteratively.

Theoretically, the training objective takes the form of the variational lower bound of log-likelihood of data:

$$\log p(G) \geq \mathcal{L}_{base} + \sum_{t=0}^T \mathcal{L}_t, \quad (5)$$

$$\mathcal{L}_{base} = -KL(q(G_T|G_0)|p(G_T)), \quad (6)$$

$$\mathcal{L}_t = KL(q(G_{t-1}|G_t)|p(G_{t-1}|G_t)). \quad (7)$$

However, it is found out that predicting the Guassian noise  $\epsilon$  makes it easier for the neural network training. Therefore,  $\mathcal{L}_t$  (Kingma et al. 2021) takes the form of

$$\mathcal{L}_t = E_{\epsilon_t \sim \mathcal{N}(0, I)} \left( \frac{1}{2} \left( 1 - \frac{\text{SNR}(t-1)}{\text{SNR}(t)} \right) \|\epsilon_t - \hat{\epsilon}_t\|^2 \right). \quad (8)$$

## Methodology

In this section, we provide details of our proposed molecule generation framework, including the E(n) equivariant denosing kernel, Geometric-Facilitated loss, the forward and reverse process, and the optimization objective. The overview of GFMDiff is shown in Fig 1. At each time step, molecule conformations are sampled as inputs. The DTN ensures complete utilization of molecule geometries by taking pair-wise distances and triplet-wise angles as inputs. These two kinds of features each stand for interatomic forces and multi-body interactions. The incorporation of GFLoss further guarantees the reasonableness and soundness of generated samples.

## Dual-Track Transformer Network

In this subsection, we elaborate on **Dual-Track Transformer Network** (DTN) as the E(n) equivariant backbone of GFMDiff. DTN is designed to effectively capture interatomic relationships and atom features. Since 3D molecular geometries possess invariance properties such as rotations, translations, reflections, and permutations, it is essential for the denoising kernel to satisfy such properties. The proposed DTN is not only E(n) equivariant, but also able to fully leverage spatial information.

In our proposed method, we regard an input molecule with the total number of atoms  $N$  as  $G = (P, X, A, V)$ , where  $P = (p_1, p_2, \dots, p_N) \in \mathbb{R}^{N \times 3}$  represents atom coordinates,  $X = (x_1, x_2, \dots, x_N) \in \mathbb{R}^{N \times nf}$  represents one-hot encoding of atomic numbers,  $A = (a_1, a_2, \dots, a_N) \in \mathbb{R}^N$  represents atomic numbers, and  $V = (v_1, v_2, \dots, v_N) \in \mathbb{R}^N$  stands for valencies of atoms. To ensure the quest for the equivariance, DTN utilizes pair-wise distances and triplet-wise angles to capture the geometry information. The Euclidean distance between atom  $i$  and  $j$ , which reflects the strength of interatomic force, is obtained by:

$$d_{ij} = \|p_i - p_j\|_2. \quad (9)$$

Given the complicated relationships among atoms during the sampling phase, simply using pair-wise distances is insufficient to excavate spatial information. Therefore, we further calculate the triplet-wise angle using:

$$\varphi_{ijk} = \arccos \left( \frac{(p_i - p_j) \times (p_i - p_k)}{\|p_i - p_j\|_2 \times \|p_i - p_k\|_2} \right). \quad (10)$$

The above geometric calculations allow us to further featurize local geometries through radius basis function (RBF) network:

$$e_{ij} = \text{Linear}(\text{RBF}(d_{ij}), e_i, e_j), \quad (11)$$

$$e_{ijk} = \text{Linear}(\text{RBF}(\varphi_{ijk}), e_i, e_j, e_k), \quad (12)$$

where  $e_i = \text{Embedding}(x_i, a_i, v_i)$  is the node embedding of atom  $i$  that combines atomic numbers and valencies. These features are later fed into DTN with  $L$  layers.

Each layer of DTN consists of the following components, an atom-pair track, a pair-triplet track, and a connection module. The atom-pair track simulates the influence of interatomic forces on atoms while the pair-triplet track models the impact of potential bond angles on edges. Just as its name implies, the connection module serves as the bridge between two tracks to promote better representation learning by injecting atom features back to pair-wise features.

The atom-pair track involves predicting influences of other atoms and interatomic forces on target atoms. The track takes atom embeddings  $e_i$  and pair embeddings  $e_{ij}$  as inputs:

$$e_i = \text{LayerNorm}(e_i), e_{ij} = \text{LayerNorm}(e_{ij}), \quad (13)$$

$$\mathbf{Q}_i = \text{Linear}(e_i), \mathbf{K}_i = \text{Linear}(e_i) + \text{Linear}(e_{ij}), \quad (14)$$

$$a_i = \text{Dropout}(\text{softmax} \frac{\mathbf{Q}_i \mathbf{K}_i^T}{\sqrt{d_h}}), \quad (15)$$

$$\mathbf{V}_i = \text{Linear}(e_{ij}) + \text{Linear}(e_i) + \text{Linear}(e_j), \quad (16)$$

$$\hat{e}_i = \text{Linear}(a_i \mathbf{V}_i^T), \quad (17)$$

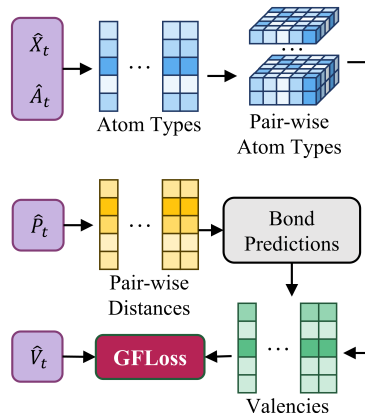


Figure 3: The illustration of GFLoss. We leverage chemical rules to predict the existence of bonds and then calculate potential valencies based on probabilities of atom types and bond predictions. The loss minimizes the difference between valencies predicted by DTN and valencies calculated from molecule geometries.

where  $d_h$  is the number of heads. Atom embeddings first get updated by adding predictions of atom-pair track and are later passed to a feed forward network. In each layer, atom absorbs aggregated representations of other atoms and corresponding atom pairs.

Similarly, the pair-triplet track predicts the impact of complex geometry substructures on interatomic forces. It is worth noting that triplet embeddings  $e_{ijk}$  does not get updated in the transformer structure, because this would significantly increase the quest for computational resources. They only get updated whenever atom coordinates are renewed.

The connection module serves as the role that fuse atom embeddings into pair embeddings. For pair embedding  $e_{ij}$ , it absorbs atomic feature information from the connection module and local spatial information from the pair-triplet track at the same time.

$$e_{ij} = \text{LayerNorm}(e_{ij} + \text{Linear}(\text{Linear}(e_i) \otimes \text{Linear}(e_j))) \quad (18)$$

In terms of the approach to update coordinates, we follow the design of PosUpdate module in EDM (Hoogeboom et al. 2022) and MDM (Huang et al. 2023). At the end of each layer, pair-wise and triplet-wise embeddings get updated since molecule conformations are altered:

$$e_{ij} = \text{Linear} \left( \text{Linear}(\text{RBF}(\hat{d}_{ij}), \hat{e}_i, \hat{e}_j) \right), \quad (19)$$

$$e_{ijk} = \text{Linear}(\text{RBF}(\hat{\varphi}_{ijk}), e_{ijk}). \quad (20)$$

## Geometric-Facilitated Loss

Predicting the existence of bonds is a fundamental and indispensable task in molecule graph generation. Unlike previous research that heavily relies on predefined rules, we propose to actively intervene in bond formation during the training process by designing a delicate training objective term

Type	Method	NLL↓	Atom Stability (%) ↑	Mol Stability (%) ↑	Validity (%) ↑	Uniqueness-Validity (%) ↑
NF	E-NF	-59.7	85.0	4.9	40.2	39.4
AR	G-SchNet	N/A	95.7	68.1	85.5	80.3
DDPM	EDM	-110.7±1.5	98.7±0.1	82.0±0.4	91.9±0.5	90.7±0.6
	Bridge+Force	N/A	98.8±0.1	84.6±0.3	N/A	N/A
	GCDM	<b>-171.0±0.2</b>	98.7±0.0	85.7±0.4	94.8±0.2	93.3±0.0
	GeoLDM	N/A	98.9±0.1	<b>89.4±0.5</b>	93.8±0.4	92.7±0.5
Ours	GFMDiff	-123.1±0.4	98.7±0.1	85.9±0.2	94.9±0.2	94.2±0.2
	w/o tri					
	GFMDiff w/o GFLoss	-127.5±0.4	98.7±0.0	86.5±0.1	95.2±0.0	94.5±0.0
	GFMDiff	-128.0±0.2	<b>98.9±0.0</b>	87.7±0.2	<b>96.3±0.3</b>	<b>95.1±0.2</b>
Data			99.0	95.2	97.7	97.7

Table 1: Performance comparison on GEOM-QM9. Results of 10000 generated samples are reported with standard deviations across 3 runs using different seeds.

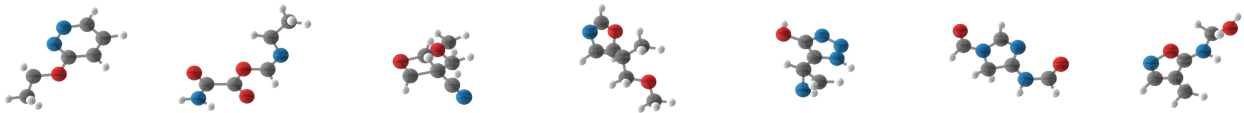


Figure 4: Molecule samples generated by GFMDiff for GEOM-QM9

named **Geometric-Facilitated Loss** (GFLoss). The intention of this loss function is to guide the model in generating molecules that not only possess valid topological structures but also stable conformations. We consider the valencies of atoms to be the an type of auxiliary features of great importance in molecule generation. Therefore, valencies of atoms are incorporated as part of atom features in the aboved metioned DTN. The cross validation of valencies allows the model to establish close connections between geometries and validity.

According to the predefined rules, atom pairs with proper distances are considered to be connected by bonds. For single, double, or triple bond, there are typical distances between certain atoms. If the distance between a pair of atoms is in certain range, these two atoms are considered to be connect by corresponding type of bond. Let the predefined distances and margins to be  $\mathbf{D} \in \mathbb{R}^{nf \times nf \times 3}$  and  $\mathbf{M} \in \mathbb{R}^3$ , where 3 stands for the number of bond types. Based on outputs of DTN  $\hat{G}_t = (\hat{P}_t, \hat{X}_t, \hat{A}_t, \hat{V}_t)$ , we first predict the probabilities of atom types using a softmax function:

$$\mathbf{p}_t(\hat{X}_{\text{atom}}) = \text{softmax}(\hat{X}_t) \in \mathbb{R}^{N \times nf}, \quad (21)$$

where  $\hat{X}_t$  here represents the predicted atom types in one-hot format with the dimension of  $nf$ . The probabilities of pair-wise atom types are

$$\mathbf{p}_t(\hat{X}_{\text{pair}}) = \mathbf{p}_t(\hat{X}_{\text{atom}}) \cdot \mathbf{p}_t(\hat{X}_{\text{atom}}) \in \mathbb{R}^{N \times N \times nf \times nf}. \quad (22)$$

With the predicted atom coordinates  $\hat{P}_t$ , pair-wise distance matrix  $\mathbf{d}_t \in \mathbb{R}^{N \times N}$  can be obtained and is expanded

to  $\mathbb{R}^{N \times N \times nf \times nf \times 3}$  for convenience. Then the margin  $\mathbf{m}_t$  between pair-wise distances and typical bond distancess is:

$$\mathbf{m}_t = \mathbf{d}_t - (\mathbf{D} + \mathbf{M}) \in \mathbb{R}^{N \times N \times nf \times nf \times 3}. \quad (23)$$

Take atom  $i$  and  $j$  for an example, suppose their chances to be Carbon are above zero, if any element in margin  $\mathbf{m}_t(i, j, \text{C}, \text{C}, :) \in \mathbb{R}^3$  is below zero, it indicates the presence of a bond between atom  $i$  and  $j$ . Specific type of bond is determined by the index of the minimum value in  $\mathbf{m}_t(i, j, \text{C}, \text{C}, :)$ . If  $\arg \min(\mathbf{m}_t(i, j, \text{C}, \text{C}, :))$  is 1, then they are connected by a single bond. They are connected by a triple bond if  $\arg \min(\mathbf{m}_t(i, j, \text{C}, \text{C}, :))$  happen to be 3. The boolean matrix that represents the existence of bonds is noted as  $\text{ISBOND}_t \in \mathbb{R}^{N \times N \times nf \times nf}$

Once we have the probabilities of pair-wise atom types and the existence of bonds, the probable valencies of atoms could be estimated as:

$$\hat{V}_{\text{pred}}(t) = \text{sum}(\mathbf{p}_t(\hat{X}_{\text{pair}}) \odot \text{ISBOND}_t) \in \mathbb{R}^N. \quad (24)$$

Since input data are fused with different level of noises, GFLoss is fomulated as the mean square error between the predicted valencies  $V_{\text{pred}}$  and the ground-truth valencies  $V$ :

$$\mathcal{L}_t = E_{\epsilon_t \sim \mathcal{N}(0, I)} \left( \frac{1}{2} \omega(t) (|\epsilon_t - \hat{\epsilon}_t|^2 + \lambda \mathcal{L}_{GF}(t)) \right), \quad (25)$$

$$\mathcal{L}_{GF}(t) = \|\alpha_t (\hat{V}_{\text{pred}}(t) - V_t)\|^2, \quad (26)$$

where  $\alpha_t$  is the level of ground-truth data in a piece of noisy input in diffusion process and  $\omega(t) = (1 - \text{SNR}(t)) / \text{SNR}(t - 1)$ .

Task	$\alpha$	$\Delta\varepsilon$	$\varepsilon_{\text{HOMO}}$	$\varepsilon_{\text{LUMO}}$	$\mu$	$C_v$
Units	Bohr <sup>3</sup>	meV	meV	meV	D	$\frac{\text{cal}}{\text{mol}}\text{K}$
Naïve (Upper-bound)	9.01	1470	645	1457	1.616	6.857
# Atom	3.86	866	426	813	1.053	1.971
EDM	2.76	655	356	584	1.111	1.101
GCDM	<u>1.97</u>	602	344	479	<u>0.844</u>	<u>0.689</u>
GeoLDM	2.37	<u>587</u>	<u>340</u>	522	1.108	1.025
GFMDiff	<b>1.74</b>	<b>558</b>	<b>321</b>	<b>430</b>	<b>0.728</b>	<b>0.593</b>
QM9 (Lower-bound)	0.10	64	39	36	0.043	0.040

Table 2: Performance comparison for conditioned molecule generation on QM9. With conditioned samples, Results are in the form of mean absolute error (MAE) for property prediction of 10000 conditional samples by an EGNN classifier.

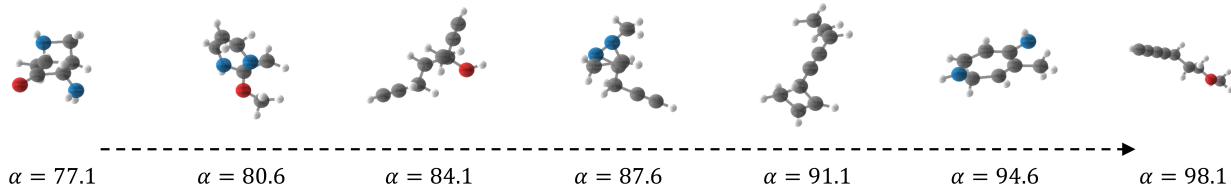


Figure 5: Generated samples of GFMDiff on QM9 conditioned with increasing values of  $\alpha$

## Experiments

In this section, we report the performance comparison of GFMDiff on GEOM-QM9 (Ramakrishnan et al. 2014) and GEOM-Drugs (Axelrod and Gomez-Bombarelli 2022). Results on three current benchmarks indicate that our method outperforms state-of-the-art (SOTA) models in multiple aspects.

### Setup

In order to make comprehensive comparisons, we conduct experiments on two benchmark datasets in molecule generation: GEOM-QM9 (Ramakrishnan et al. 2014) and GEOM-Drugs (Axelrod and Gomez-Bombarelli 2022). GEOM-QM9 dataset consists of over 130K molecules and their corresponding conformations, where molecules have 18 atoms with hydrogen included on average. GEOM-Drugs includes over 450K molecules and 37M conformations, where size of molecule is 44 on average.

To assess the performance of GFMDiff in a fair and comprehensive manner, we compare it against six representative baselines in this field, which are E-NF (Garcia Satorras et al. 2021), G-SchNet (Gebauer, Gastegger, and Schütt 2019), EDM (Hoogeboom et al. 2022), models of Wu et al. (Gong et al. 2022), GCDM (Morehead and Cheng 2023), and GeoLDM (Xu et al. 2023). We refer to the performances of the first three models stated in EDM, as well as results of the remaining baselines reported in GCDM and GeoLDM.

In terms of evaluation metrics, we adopt the same ones used in previous research, which are stability, validity, and uniqueness. Stability measures the proportion of atoms with correct valencies and molecules whose atoms are all stable. Validity is defined as the percentage of molecules that are theoretically correct and uniqueness shows the probability

of non-repetitive samples. Arrows in Table 1 and Table 3 signify the preferred direction of each criteria. The best results are highlighted in bold and the second best results are underlined.

### De Novo Molecule Generation on QM9

In order to analyze results fairly, we use the same dataset settings as previous methods. To evaluate the effectiveness of GFLoss and triplet geometric information learning, we include GFMDiff w/o GFLoss and GFM w/o tri for comparison. In GFM w/o tri, we replace the pair-triplet track multi-head attention module with a self-attention module of pair-wise features. The weight for GFLoss  $\lambda$  is set 0.01. On QM9, GFMDiff is trained for around 1000 epochs, with a five layer DTN and the embedding size of 256.

As it is shown in Table 1, GFMDiff outperforms all baselines and achieves the best performance in stability, validity, and uniqueness times validity. GFMDiff and recent SOTA methods show no major difference in stability of atoms, but the performance lead of GFMDiff over the second-best method using the same generative methods in terms of stability of molecules is 2.1%. This indicates that our model is capable of generating stable molecules. We believe that the molecule stability could be further improved using latent diffusion in GeoLDM. The performance lead of GFMDiff over the SOTA method in validity and validity times uniqueness is 1.1% and 1.3%, respectively. The superior performance in validity means that GFMDiff generates molecules not only with accurate conformations, but also with correct valid and unique structures. It is intriguing to find out that GFMDiff exhibits lower performance in terms of the negative log-likelihood of data (NLL) compared to GCDM, but still surpasses other baselines. A possible explanation could

Type	Method	Atom Stable (%) $\uparrow$	Mol Stable (%) $\uparrow$
Normalizing flow	E-NF	75.0	0
	EDM	81.3	0.0
DDPM	Bridge+Force	82.4 $\pm$ 0.8	0.0
	GCDM	86.4 $\pm$ 0.2	3.7 $\pm$ 0.3
	GeoLDM	84.4	3.2
	Ours	<b>86.5<math>\pm</math>0.2</b>	<b>3.9<math>\pm</math>0.2</b>
Data		86.5	2.8

Table 3: Performance comparison on GEOM-Drugs. Results of 10000 generated samples are reported with standard deviations across 3 runs using different seeds.

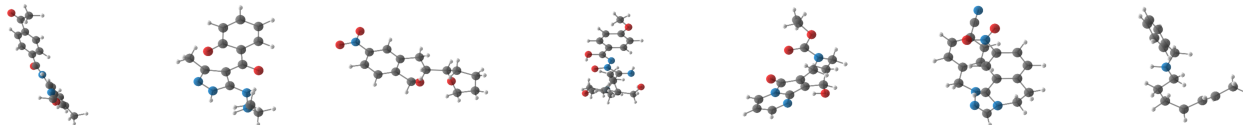


Figure 6: Molecule samples generated by GFMDiff for GEOM-Drugs

be the different ways of applying geometric information between GFMDiff and GCDM.

Moreover, the ablations of GFLoss and triplet-wise geometry illustrate the effectiveness of them. Among GFMDiff and its ablation models, GFMDiff w/o tri achieves the lowest results. This means the incorporation of complete local geometry information contributes more to the performance lift than GFLoss. In summary, GFMDiff exhibits the ability to generate stable molecules while addressing validities of samplessimultaneously.

### Conditional Molecule Generation on GEOM-QM9

For conditional molecule generation on QM9, we compare our GFMDiff with existing methods along with naive baselines. In Table 2, we show the comparison of MAE on property prediction task. The "Naive (Upper-bound)" is a baseline where samples and labels are shuffled and the "#Atoms" is the property prediction method which simply relies of the number of atoms. Lower mean absolute errors of a model than these two baselines indicate the model is capable to incorporate properties and molecule conformation information into generated samples.

As it is demonstrated in Table 2, our methods outperforms the state-of-the-art method in this task. Samples of samples with various values of  $\alpha$  is shown in Figure 5 as well. The performance lead of GFMDiff over the second-best method on for 6 properties are 11.7%, 4.9%, 6.2%, 10.2%, 13.7%, and 13.9%, respectively. Results indicates the superiority of our GFMDiff in generate molecules with desirable properties.

### De Novo Molecule Generation on GEOM-Drugs

It is a challenging task to generate molecules for GEOM-Drugs dataset, since it is a large scale dataset of big molecules with up to 181 atoms. The relatively large scale of molecules and low stabilities of ground truth data bring

huge challenges to 3D molecule generation. In experiments on GEOM-Drugs, we compares GFMDiff with E-NF, EDM, Bridge + Force, GCDM, and GeoLDM. Since current methods performs poorly in the novelty of molecules, we only list the stability of generated samples for comparison.

Due to the size of molecules in GEOM-Drugs, the stability of ground truth data are much lower than that in QM9. The proposed GFMDiff outperforms GCDM in terms of atom stability by a small margin, while GFMDiff outperforms the second-best result on molecule stability by 5.4%. It's worth noting that GeoLDM, which generates samples with high stabilities on QM9, encounters a bottleneck in generating large molecules. Some samples generated by GFMDiff are shown in Figure 6. Results on Drugs also demonstrate the capability of our proposed GFMDiff to generate stable molecule geometries.

## Conclusion

In this paper, we propose GFMDiff, a novel molecule generation methods that fully excavates geometric information to help expressive representation learning and accurate bonds formation in molecule graphs. Unlike earlier methods that did not comprehensively model molecular geometries and heavily rely on predefined rules to generate bonds, GFMDiff makes full use of spatial information to assist on representation learning and facilitate accurate edge generation. We adopt DTN as the denoising kernel to update atom features and coordinates based on interatomic forces and multi-body interactions. The GFLoss is also implemented to actively intervene the formation of bonds during each time step at the training stage. We conduct comprehensive experiments to evaluate the effectiveness and performance edge of the proposed techniques over SOTA methods. It is shown that GFMDiff is capable to generate valid molecules with accurate conformations and correct atom valencies.

## Acknowledgments

This project is supported by National Key Research and Development Program of China (2022YFB4500300), the National Natural Science Foundation of China (72273132), in part by Key Research Project of Zhejiang Lab (No. 2022PI0AC01). We also gratefully acknowledge the valuable comments from anonymous reviewers.

## References

- Avrahami, O.; Lischinski, D.; and Fried, O. 2022. Blended Diffusion for Text-Driven Editing of Natural Images. In *Proceedings of the IEEE/CVF Conference on Computer Vision and Pattern Recognition (CVPR)*, 18208–18218.
- Axelrod, S.; and Gomez-Bombarelli, R. 2022. GEOM, energy-annotated molecular conformations for property prediction and molecular generation. *Scientific Data*, 9(1): 185.
- Cai, R.; Yang, G.; Averbuch-Elor, H.; Hao, Z.; Belongie, S.; Snavely, N.; and Hariharan, B. 2020. Learning Gradient Fields for Shape Generation. In Vedaldi, A.; Bischof, H.; Brox, T.; and Frahm, J.-M., eds., *Computer Vision – ECCV 2020*, 364–381. Cham: Springer International Publishing. ISBN 978-3-030-58580-8.
- Dabral, R.; Mughal, M. H.; Golyanik, V.; and Theobalt, C. 2023. Mofusion: A Framework for Denoising-Diffusion-Based Motion Synthesis. In *Proceedings of the IEEE/CVF Conference on Computer Vision and Pattern Recognition (CVPR)*, 9760–9770.
- Dinh, L.; Krueger, D.; and Bengio, Y. 2015. NICE: Non-linear Independent Components Estimation. arXiv:1410.8516.
- Garcia Satorras, V.; Hoogeboom, E.; Fuchs, F.; Posner, I.; and Welling, M. 2021. E(n) Equivariant Normalizing Flows. In Ranzato, M.; Beygelzimer, A.; Dauphin, Y.; Liang, P.; and Vaughan, J. W., eds., *Advances in Neural Information Processing Systems*, volume 34, 4181–4192. Curran Associates, Inc.
- Gebauer, N.; Gastegger, M.; and Schütt, K. 2019. Symmetry-adapted generation of 3d point sets for the targeted discovery of molecules. In Wallach, H.; Larochelle, H.; Beygelzimer, A.; d'Alché-Buc, F.; Fox, E.; and Garnett, R., eds., *Advances in Neural Information Processing Systems*, volume 32. Curran Associates, Inc.
- Gong, C.; Wu, L.; Liu, X.; Ye, M.; and qiang liu. 2022. Diffusion-based Molecule Generation with Informative Prior Bridges. In *NeurIPS 2022 AI for Science: Progress and Promises*.
- Goodfellow, I.; Pouget-Abadie, J.; Mirza, M.; Xu, B.; Warde-Farley, D.; Ozair, S.; Courville, A.; and Bengio, Y. 2014. Generative Adversarial Nets. In Ghahramani, Z.; Welling, M.; Cortes, C.; Lawrence, N.; and Weinberger, K., eds., *Advances in Neural Information Processing Systems*, volume 27. Curran Associates, Inc.
- Ho, J.; Jain, A.; and Abbeel, P. 2020. Denoising Diffusion Probabilistic Models. In Larochelle, H.; Ranzato, M.; Hassel, R.; Balcan, M.; and Lin, H., eds., *Advances in Neural Information Processing Systems*, volume 33, 6840–6851. Curran Associates, Inc.
- Ho, J.; Saharia, C.; Chan, W.; Fleet, D. J.; Norouzi, M.; and Salimans, T. 2022. Cascaded Diffusion Models for High Fidelity Image Generation. *Journal of Machine Learning Research*, 23(47): 1–33.
- Hoogeboom, E.; Nielsen, D.; Jaini, P.; Forré, P.; and Welling, M. 2021. Argmax Flows and Multinomial Diffusion: Learning Categorical Distributions. In Ranzato, M.; Beygelzimer, A.; Dauphin, Y.; Liang, P.; and Vaughan, J. W., eds., *Advances in Neural Information Processing Systems*, volume 34, 12454–12465. Curran Associates, Inc.
- Hoogeboom, E.; Satorras, V. G.; Vignac, C.; and Welling, M. 2022. Equivariant Diffusion for Molecule Generation in 3D. In *Proceedings of the 39th International Conference on Machine Learning*, volume 162 of *Proceedings of Machine Learning Research*, 8867–8887. PMLR.
- Huang, L.; Zhang, H.; Xu, T.; and Wong, K.-C. 2023. Mdm: Molecular diffusion model for 3d molecule generation. In *Proceedings of the AAAI Conference on Artificial Intelligence*, volume 37, 5105–5112.
- Kingma, D.; Salimans, T.; Poole, B.; and Ho, J. 2021. Variational Diffusion Models. In Ranzato, M.; Beygelzimer, A.; Dauphin, Y.; Liang, P.; and Vaughan, J. W., eds., *Advances in Neural Information Processing Systems*, volume 34, 21696–21707. Curran Associates, Inc.
- Kingma, D. P.; and Welling, M. 2022. Auto-Encoding Variational Bayes. arXiv:1312.6114.
- Lei, J.; Deng, C.; Shen, B.; Guibas, L.; and Daniilidis, K. 2023. NAP: Neural 3D Articulated Object Prior. In *Thirty-seventh Conference on Neural Information Processing Systems*.
- Luo, S.; and Hu, W. 2021. Score-Based Point Cloud Denoising. In *Proceedings of the IEEE/CVF International Conference on Computer Vision (ICCV)*, 4583–4592.
- Morehead, A.; and Cheng, J. 2023. Geometry-Complete Diffusion for 3D Molecule Generation. In *ICLR 2023 - Machine Learning for Drug Discovery workshop*.
- Niu, C.; Song, Y.; Song, J.; Zhao, S.; Grover, A.; and Ermon, S. 2020. Permutation Invariant Graph Generation via Score-Based Generative Modeling. In Chiappa, S.; and Calandra, R., eds., *Proceedings of the Twenty Third International Conference on Artificial Intelligence and Statistics*, volume 108 of *Proceedings of Machine Learning Research*, 4474–4484. PMLR.
- Ramakrishnan, R.; Dral, P. O.; Rupp, M.; and Von Lilienfeld, O. A. 2014. Quantum chemistry structures and properties of 134 kilo molecules. *Scientific Data*, 1(1): 1–7.
- Ronneberger, O.; Fischer, P.; and Brox, T. 2015. U-Net: Convolutional Networks for Biomedical Image Segmentation. In Navab, N.; Hornegger, J.; Wells, W. M.; and Frangi, A. F., eds., *Medical Image Computing and Computer-Assisted Intervention – MICCAI 2015*, 234–241. Cham: Springer International Publishing. ISBN 978-3-319-24574-4.
- Savinov, N.; Chung, J.; Binkowski, M.; Elsen, E.; and van den Oord, A. 2022. Step-unrolled Denoising Autoencoders for Text Generation. In *International Conference on Learning Representations*.



Shabani, M. A.; Hosseini, S.; and Furukawa, Y. 2023. HouseDiffusion: Vector Floorplan Generation via a Diffusion Model With Discrete and Continuous Denoising. In *Proceedings of the IEEE/CVF Conference on Computer Vision and Pattern Recognition (CVPR)*, 5466–5475.

Song, Y.; and Ermon, S. 2019. Generative Modeling by Estimating Gradients of the Data Distribution. In Wallach, H.; Larochelle, H.; Beygelzimer, A.; d'Alché-Buc, F.; Fox, E.; and Garnett, R., eds., *Advances in Neural Information Processing Systems*, volume 32. Curran Associates, Inc.

Song, Y.; Sohl-Dickstein, J.; Kingma, D. P.; Kumar, A.; Ermon, S.; and Poole, B. 2021. Score-Based Generative Modeling through Stochastic Differential Equations. In *International Conference on Learning Representations*.

Vignac, C.; Krawczuk, I.; Siraudin, A.; Wang, B.; Cevher, V.; and Frossard, P. 2023a. DiGress: Discrete Denoising diffusion for graph generation. In *International Conference on Learning Representations*.

Vignac, C.; Osman, N.; Toni, L.; and Frossard, P. 2023b. MiDi: Mixed Graph and 3D Denoising Diffusion for Molecule Generation. In *ICLR 2023 - Machine Learning for Drug Discovery workshop*.

Xu, M.; Powers, A. S.; Dror, R. O.; Ermon, S.; and Leskovec, J. 2023. Geometric Latent Diffusion Models for 3D Molecule Generation. In *Proceedings of the 40th International Conference on Machine Learning*, volume 202 of *Proceedings of Machine Learning Research*, 38592–38610. PMLR.

Yuan, Z.; Zhang, Y.; Tan, C.; Wang, W.; Huang, F.; and Huang, S. 2023. Molecular Geometry-aware Transformer for accurate 3D Atomic System modeling. arXiv:2302.00855.